On Statistical Interference Modeling and Deployment Issues for Cognitive Radio Systems in Shadow Fading Environments

Muhammad Fainan Hanif, Peter J. Smith and Pawel A. Dmochowski

Abstract

In this paper we deal with the issues of statistical modeling of the aggregate interference due to cognitive radios (CRs) at primary users and the deployment of CR systems in real world environments. We explore the possibilities of modeling the interference by two and three-parameter log-normal distributions. We find that the traditional approach of using a two-parameter log-normal is not a suitable option on account of the massive skewness difference between the actual interference and the log-normal variable used for fitting purposes. Similarly, we observe that the recently proposed three-parameter log-normal approximation works only under specific scenarios. While probing these issues, we also arrive at a considerably simpler way of deriving the cumulants of the total interference. Due to analytical difficulties, we resort to simulations to assess different CR deployment schemes. Based on CRs equipped with apriori knowledge of the radio environment map (REM), we compare various CR system design parameters achieved by the proposed techniques. Furthermore, we describe the effect of imperfections in the REM information on the performance of CR systems. Via analysis and simulations we explore the relationship between the required precision of the REM and various system properties.

Index Terms

Cognitive radio networks, interference statistics, fading channel, radio environment map, primary exclusion zone.

A subset of this work was presented at the IEEE ICC [1] and IEEE AusCTW [2].
M. F. Hanif is with the Centre for Wireless Communications, University of Oulu, Finland (e-mail: mhanif@ee.oulu.fi, mfh21@uclive.ac.nz). P. J. Smith is with the Department of Electrical and Computer Engineering, University of Canterbury, Christchurch, New Zealand (email: peter.smith@canterbury.ac.nz). P. A. Dmochowski is with the School of Engineering and Computer Science, Victoria University of Wellington, New Zealand (e-mail: pawel.dmochowski@ecs.vuw.ac.nz).

I. Introduction

With the ever increasing demand for wireless devices, the conventional methodology of granting exclusive licences to service providers to operate in a particular frequency band appears inadequate. This inflexible approach has led to perceived scarcity of the precious radio-frequency (RF) spectrum. Results of various measurement campaigns conducted worldwide, for example [3], [4], also reveal that the contemporary obdurate frequency allocation philosophy is responsible for the inefficient usage of expensive RF spectrum. This lack of efficient spectrum usage has sparked a tremendous research effort on the concept of cognitive radios (CRs) or, loosely speaking, secondary users (SUs). The CRs are being considered as intelligent radio nodes capable of opportunistically using RF spectrum while harmoniously co-existing with the primary (licensed) users (PUs). Realizing the potential benefits of introducing CRs, the IEEE has formed a special working group (IEEE 802.22) to develop an air interface for opportunistic secondary access to the TV spectrum.

The CRs should try their best to protect the PUs from their adverse interference. Hence, a considerable research effort has focused on CR signal processing to avoid interference at the PU and this includes cases where the CR has correctly identified a free channel [5]. However, such efforts may jeopardize the quality of service (QoS) operation expected from the cognitive devices. In general, CR performance is at risk due to PU interference demands and also through PU interference at the CR, where interference reduction methods may be needed [6]. Accurate spectrum sensing capabilities are being developed [7] for CRs and it is envisaged that either individually, or via collaboration, the secondary devices will be able to detect the licensed users with an acceptably low probability of failure. It is evident that the statistics of the interfering signals will play an important role in the design of CR systems. Thus, modeling the total CR interference is an important issue. Various results [8], [9] have appeared in this regard. [9] models the combined interference with heavy-tailed α-stable distributions in an *infinite* field of interferers. [8] proposes a 3-parameter lognormal to accomplish this task. Later in the paper we show that this approach is applicable only in certain scenarios.

In addition to sensing techniques, a number of schemes aimed at avoiding harmful interference have recently been developed, either based on a *primary exclusion zone* (PEZ) approach [10] or on the exploitation of *radio environment map* (REM) [11] information. The former utilizes the knowledge of interference statistics to define an exclusion zone inside which CRs are not permitted to operate, while the latter, which assumes a more complete knowledge of the interferers including their geographical

position, permits only selected CRs in order to maintain a specific signal-to-interference-and-noise ratio (SINR).It is thus necessary to characterize the nature of the interfering signals along with their impact on the performance of the incumbent licensed users. In addition, the amount of access that CRs are able to obtain without too much impact on the PU is a key issue.

Contributions: Our contributions include the following. We derive the cumulative distribution function (CDF) of the interference due to a cognitive device assuming lognormal shadowing and path loss effects and investigate the nature of the distribution of the total interference due to multiple CRs. We derive a simplified expression for the cumulants of the total interference, which are in turn used in approximating the interference with a shifted lognormal distribution and determining the scenarios of applicability of this approach. PEZs are compared in which CRs are not permitted to operate. The PEZ approach allows access to CRs when the primary device is willing to pay a price in the form of a reduction in its threshold signal to noise ratio (SNR). We determine the permissible number of CRs when the REM is *apriori* known to the CRs and establish how these numbers vary in different fading environments. In the presence of coarse REM information we show that when the REM for a given area is discretized then the total CR interference is significantly underestimated when realistic grid sizes are considered. We also determine the interaction between shadow fading correlation and REM grid size and evaluate their impact on interference estimation. Finally, we determine the scenarios (CR density, fading parameters) under which REM equipped CR systems outperform PEZ based cognitive wireless systems. To the best of our knowledge, we present the first comparative study of the PEZ and the proposed REM schemes with and without perfect REM information in shadowing environments. Of particular novelty in this paper is the comparison of centralized with decentralized selection and the consideration of a finite grid size REM, complete with an analysis of grid size and optimal grid interpolation. In addition, the analytical work clarifies the need for interference modeling which goes beyond the scope of standard or extended lognormal approximations.

The remainder of this paper is organized as follows: Section II describes the system model. Section III characterizes the interference seen by a PU receiver. Specifically, the CDF of the interference due to a single CR is derived, and the case of multiple CRs is discussed. We introduce the PEZ and REM schemes in Section IV, including a discussion of modeling the REM imperfections. We evaluate the performance via simulation in Section V. Finally, Section VI presents concluding remarks.

II. System Model

In the system model we consider a PU receiver in the center of a circular region of radius R. The PU transmitter is located uniformly in an annulus of outer radius R and inner radius R_0 centered on the PU receiver. It is to be noted that we place the PU receiver at the center only for the sake of mathematical convenience. The use of the annulus restricts devices from being too close to the receiver. This matches physical reality and also avoids problems with the classical inverse power law relationship between signal strength and distance [12]. In particular, having a minimum distance, R_0, prevents the signal strength from becoming infinite as the transmitter approaches the receiver. Similarly, we assume that multiple CR transmitters are uniformly located in the annulus. At any given time, each CR has a probability of seeking a connection, given by the activity factor, p. The number of CRs wishing to operate is denoted N_{CR}. Of these CRs, a certain number will be accepted depending on the allocation mechanism. Hence, a random number of CRs denoted $N \leq N_{CR}$ will transmit during the PU transmission and create interference at the PU receiver.

The received signal strength for both the PU transmitter to PU receiver and CR transmitter to PU receiver is assumed to follow the classical distance dependent, lognormal shadowing model. For a generic interferer, this is given by

$$I = BLr^{-\gamma} = B10^{\tilde{X}/10}r^{-\gamma} = Be^{X}r^{-\gamma}, \tag{1}$$

where r is the random distance from the transmitter to the receiver, γ is the path loss exponent (normally in the range of 2 to 4) and L is a shadow fading variable. The lognormal variable, L, is given in terms of the zero mean Gaussian, $\tilde{X}$, which has standard deviation σ (dB) and $X = \beta\tilde{X}$ where $\beta = \log(10)/10$. The standard deviation of X is denoted by σ_x. The constant B is determined by the transmit power. The desired primary signal strength, S, has the same form, with a different transmit power, so that $S = AL_p r_p^{-\gamma}$. Note that all the links are assumed to be independent and identically distributed (i.i.d.) so that spatial correlation is ignored.

III. Statistical Characterization of Interference at the Primary Receiver

A. Interference Due to Single Cognitive User

In this section we investigate the interference at the PU receiver due to a single CR. Firstly we characterize the interfering signal, given in (1), by computing the CDF, $F_I(x) = P(I < x)$. This can

be done as follows

$$\begin{aligned} F_I(x) &= P\Big(Be^X r^{-\gamma} < x\Big) = P\left(e^{-X} r^{\gamma} > \frac{B}{x}\right) \\ &= P(e^U r^{\gamma} > y) = E_U\Big(P\Big(r > y^{\frac{1}{\gamma}} e^{\frac{-U}{\gamma}}\Big)\Big) \\ &= E_U\Big(1 - F_R\Big(y^{\frac{1}{\gamma}} e^{\frac{-U}{\gamma}}\Big)\Big). \end{aligned} \tag{2}$$

In (2), $U = -X$, E_U represents expectation over the random variable U, $y = B/x$ and $F_R(x) = P(r < x)$ is the CDF of r. To evaluate the expectation in (2) we note that the CDF of r is given by

$$F_R(r) = \frac{r^2 - R_0^2}{R^2 - R_0^2}, \qquad R_0 \leq r \leq R. \tag{3}$$

Using this CDF, (2) can be rewritten as

$$F_I(x) = E_U(G_R(U, y)), \tag{4}$$

where

$$G_R(U, y) = \begin{cases} 0 & U < w_0 \\ \left(\frac{R^2 - y^{\frac{2}{\gamma}} e^{\frac{-2u}{\gamma}}}{R^2 - R_0^2}\right) & w_0 < U < w_1 \\ 1 & U > w_1, \end{cases} \tag{5}$$

and $w_0 = \log(yR^{-\gamma})$, $w_1 = \log(yR_0^{-\gamma})$. Since $U = -X$ is Gaussian, $U \sim \mathcal{N}(0, \sigma_x^2)$, with probability density function (PDF) $f(u)$, the CDF, $F_I(x) = E_U(G_R(U, y))$, becomes

$$\begin{aligned} F_I(x) &= \int_{w_0}^{w_1} \frac{R^2 - y^{\frac{2}{\gamma}} e^{\frac{-2u}{\gamma}}}{R^2 - R_0^2} f(u)du + \int_{w_1}^{\infty} f(u)du \\ &= \frac{R^2}{(R^2 - R_0^2)\sqrt{2\pi\sigma_x^2}} \int_{w_0}^{w_1} e^{\frac{-u^2}{2\sigma_x^2}} du - \frac{(\frac{B}{x})^{2/\gamma}}{(R^2 - R_0^2)\sqrt{2\pi\sigma_x^2}} \int_{w_0}^{w_1} e^{\frac{-2u}{\gamma} - \frac{-u^2}{2\sigma_x^2}} du + \frac{1}{\sqrt{2\pi\sigma_x^2}} \int_{w_1}^{\infty} e^{\frac{-u^2}{2\sigma_x^2}} du. \end{aligned} \tag{6}$$

All the integrals in (6) can be written in terms of integrals of Gaussian PDFs. Hence, (6) reduces to

$$\begin{aligned} F_I(x) = 1 - F_Z\left(\frac{w_1}{\sigma_x}\right) + \frac{1}{R^2 - R_0^2}\Bigg[\Bigg\{R^2 F_Z\Big(\frac{w_1}{\sigma_x}\Big) - R^2 F_Z\Big(\frac{w_0}{\sigma_x}\Big)\Bigg\} \\ - \Big(\frac{B}{x}\Big)^{\frac{2}{\gamma}} e^{\left(\frac{2\sigma_x^2}{\gamma^2}\right)} \Bigg\{F_Z\left(\frac{w_1 + 2\sigma_x^2/\gamma}{\sigma_x}\right) - F_Z\left(\frac{w_0 + 2\sigma_x^2/\gamma}{\sigma_x}\right)\Bigg\}\Bigg], \end{aligned} \tag{7}$$

where $F_Z(.)$ is the CDF of a standard Gaussian. The analytical results given in (7) were found to be in

perfect agreement with Monte Carlo simulations (shown in Fig. 1) for a range of physical parameters. Next, we consider multiple CRs.

B. Interference Due to Multiple Cognitive Radios

In cognitive wireless networks the PU device under consideration may be affected by the interference due to many CRs. In this case, the total interference, denoted I_T, is given by

$$I_T = \sum_{i=1}^{N} Be^{X_i} r_i^{-\gamma} = \sum_{i=1}^{N} BL_i r_i^{-\gamma}, \tag{8}$$

where the parameters are as defined in (1). Equation (8) is a random sum of a finite number of lognormals with each lognormal being multiplied by a random distance factor. Problems similar to this, but involving a non random sum without incorporating the random distance factor, have been tackled in the past [13]–[19]. Historically, lognormal approximations to this summation have been envisaged. Approximations are definitely required since although (7) gives an analytical result for a single interferer, it is too complex to allow an exact approach for sums of interferers. Hence, one is tempted to use the same lognormal approximation for (8). However, as described below, we show that lognormal approximations are not accurate. For convenience, consider a lognormal approximation to a single interferer, I, of the form given in (1). Let the moments of I be denoted by $E(I^j) = m_j$. We seek to approximate I with the lognormal $Y = e^Z$ where $Z \sim \mathcal{N}(\mu_z, \sigma_z^2)$. The simplest approach to fitting Y is via the Fenton-Wilkinson approach [13], [15] which computes the first two moments, so that

$$E(Y^k) = E(I^k) = m_k, \quad k = 1, 2. \tag{9}$$

Hence, the lognormal approximation has perfect moments up to order 2. To demonstrate the lack of fit we consider the skewness of Y and I which also involves the third moment. For any lognormal, say Y, the third moment is related to the first two by

$$E(Y^3) = \left(\frac{E(Y^2)}{E(Y)} \right)^3. \tag{10}$$

Now, consider the skewness of I,

$$\begin{aligned} SK(I) &= \frac{E((I - m_1)^3)}{(m_2 - m_1^2)^{3/2}} \\ &= \frac{m_3 + 2m_1^3 - 3m_1 m_2}{(m_2 - m_1^2)^{3/2}}. \end{aligned} \tag{11}$$

Similarly, the skewness of Y can be written as

$$\begin{aligned} SK(Y) &= \frac{E(Y^3) + 2E(Y)^3 - 3E(Y)E(Y^2)}{(E(Y^2) - E(Y)^2)^{3/2}} \\ &= \frac{E(Y^3) + 2m_1^3 - 3m_1 m_2}{(m_2 - m_1^2)^{3/2}}. \end{aligned} \tag{12}$$

Hence, the lognormal approximation is more skewed than the real interference if $E(Y^3) > m_3$. Now, consider

$$\begin{aligned} \frac{E(Y^3)}{m_3} &= \frac{(m_2/m_1)^3}{m_3} \\ &= \frac{\left(\frac{B^2 E(e^{2X})E(r^{-2\gamma})}{BE(e^X)E(r^{-\gamma})}\right)^3}{B^3 E(e^{3X})E(r^{-3\gamma})} \\ &= \frac{\left(\frac{E(e^{2X})}{E(e^X)}\right)^3}{E(e^{3X})} \frac{\left(\frac{E(r^{-2\gamma})}{E(r^{-\gamma})}\right)^3}{E(r^{-3\gamma})} \\ &= \frac{\left(\frac{E(r^{-2\gamma})}{E(r^{-\gamma})}\right)^3}{E(r^{-3\gamma})}. \end{aligned} \tag{13}$$

The above results follow since (10) also holds for the lognormal e^X. The moments of r in (13) can be found as

$$E(r^{-k\gamma}) = \frac{2(R^{2-k\gamma} - R_0^{2-k\gamma})}{(R^2 - R_0^2)(2 - k\gamma)}. \tag{14}$$

Equation (14) is obtained using (3) as the CDF of r to compute the PDF and hence the moments. For large R (1000 m in our case), small R_0 (we use 1 m) and with $\gamma \geq 3$, (14) gives

$$E(r^{-k\gamma}) \approx \frac{-1}{R^2}\left(\frac{2}{2 - k\gamma}\right) = \frac{2}{R^2(k\gamma - 2)}. \tag{15}$$

Thus, the ratio of the moments in (13) becomes:

$$\frac{E(Y^3)}{m_3} \approx \left(\frac{\gamma - 2}{2\gamma - 2}\right)^3 \frac{R^2(3\gamma - 2)}{2}. \tag{16}$$

It can be observed from the above expression that for typical values of the parameters, $E(Y^3) >> m_3$, and the ratio is of the order of R^2. Thus the equivalent lognormal will be massively more skewed than the real interference. As skewness is a key shape determining factor (especially in the tails), the simple lognormal approximation will not be accurate. Note that this large discrepancy in skewness is due to

the random distance factors. Exactly the same conclusions are reached when attempting to fit sums of interferers. Hence, it appears that a simple lognormal approximation will not suffice and further research is required. An alternate approach, one considered by [8], is to approximate interference of the form given in (8) with a *three parameter* lognormal random variable using cumulant matching. Such an approximation was shown to be highly accurate under typical operating conditions. The parameters of the distribution can be expressed in terms of the cumulants of the interference which is now denoted $I_{T,N}$ to represent the dependence on the random number of interferers, N. For the sake of analytical tractability, instead of using a binomial random variable to model the interfering CRs, we use a Poisson random variable noting that the Poisson distribution is a limiting case of the binomial. These cumulants can be calculated by modeling the interferers by a marked Poisson process and invoking Campbell's theorem [20]. In what follows we provide a significantly simplified and more intuitive method of calculating the cumulants of $I_{T,N}$ than the one presented in [8]. We begin by noting that the moment generating function (MGF) of $I_{T,N}$ can be expressed as a function of the MGF of I by means of conditioning on N. Hence,

$$\begin{aligned}\Phi_{I_{T,N}}(s) &= E(e^{sI_{T,N}}) \\ &= \sum_{n=0}^{\infty} E(e^{sI_{T,N}}|N=n)P(N=n) \\ &= \sum_{n=0}^{\infty} E(e^{sI_{T,n}})P(N=n) \\ &= \sum_{n=0}^{\infty} \left(\Phi_I(s)\right)^n P(N=n), \end{aligned} \tag{17}$$

where the last equality assumes independent and identically distributed (i.i.d.) interferers. We recognize that (17) is in the form of the *probability generating function* (PGF) of N, and thus

$$\Phi_{I_{T,N}}(s) = G_N\left(\Phi_I(s)\right), \tag{18}$$

where the PGF, G_N, for a Poisson distributed N with mean λ is given by

$$G_N(s) = e^{\lambda(s-1)}. \tag{19}$$

Before proceeding forward, we make an important remark. Using (19) one may be tempted to obtain the *exact* distribution of the cumulative interference. For example, it is plain to see that the characteristic

function [1] of this variable is $\Phi_{I_{T,N}}(jt) = \exp\left(\lambda(\Phi_I(jt) - 1)\right)$, where $j = \sqrt{-1}$. Further, the characteristic function of the individual interferer is given by

$$\Phi_I(jt) = E(e^{jtBe^X r^{-\gamma}}) = \int_{R_0}^{R}\int_{-\infty}^{\infty} e^{jtBe^x r^{-\gamma}} f(x) f_R(r) dx dr, \tag{20}$$

where $f(x)$ is the PDF of a $\mathcal{N}(0, \sigma_x^2)$ variable and $f_R(r)$ can be obtained by differentiating (3). With the CDF given in (7), it is easy to see that (20) may not be representable in terms of elementary functions or may not even allow a closed form solution. On top of this, evaluating the inverse Fourier transform of $\Phi_{I_{T,N}}(jt)$ may be a very difficult, if not an impossible, task. Thus the motivation behind fitting a simple distribution. We note that some progress is possible using stable distributions [9] but this requires the assumptions that $R_0 \to 0$ and $R \to \infty$ giving rise to an infinite field of interferers.

Coming back to (19), we see that using (18) and (19) we can obtain the kth cumulant κ_k of $I_{T,N}$ as

$$\begin{aligned}
\kappa_k &= \left[\frac{\partial^k}{\partial s^k} \ln \Phi_{I_{T,N}}(s)\right]_{s=0} \\
&= \lambda \left[\frac{\partial^k}{\partial s^k} \Phi_I(s)\right]_{s=0} \\
&= \lambda E\left(I^k\right). \qquad (21)
\end{aligned}$$

Thus, the cumulants of the aggregate interference can be easily obtained from the moments of the individual interferers. [2] Using (1), (14) and the moments of a lognormal, the cumulants in (21) can be given as

$$\kappa_k = \lambda B^k e^{k^2\sigma_x^2/2}\left(\frac{2}{2 - k\gamma}\right)\left(\frac{R^{2-k\gamma} - R_0^{2-k\gamma}}{R^2 - R_0^2}\right). \tag{22}$$

Following [8] a shifted lognormal was fitted to the interference, $I_{T,N}$, by selecting the three parameters of the shifted lognormal to match the first 3 cumulants in (22). Although the fitting procedure was successful, the resulting shift parameter was found to be negative. Hence, in order to match the first 3 moments of $I_{T,N}$ the shifted lognormal yields negative interference values for some portion of the time. Investigation of this behavior showed that the negative shift is fundamentally a function of R_0. For one set of parameter settings, $R = 1000$ m, $\sigma = 8$ dB, $\gamma = 3.5$ and $\lambda = 1000$ CRs per square kilometer with an activity factor of 0.1, the percentage of the shifted lognormal distribution which is negative was found to vary from 88% for $R_0 = 1$m to 0% for $R_0 = 20$m. Thus it is clear that for small R_0 values the shifted lognormal is

[1] We use characteristics function since this function always exists even when it is not possible to evaluate the MGF.

[2] The same result can be obtained via Campbell's theorem [20], as considered by [8], by appropriately modifying the expression for finite cell radius and disregarding the sensing-related component.

completely inappropriate as a model for interference. However, for $R_0 \geq 20$ m the distribution is always positive and in this region it may be useful. Note that in [8] a high detection probability near the PU receiver's beacon means that CRs are very unlikely to be close to the PU. This is roughly equivalent to a larger R_0 value and hence in the presence of a beacon the shifted lognormal may be useful as shown in [8]. However, in this work we are not necessarily assuming a beacon is present and so the shifted lognormal is not used. Since there are problems with both simple approximation to the interference distribution, we employ simulations in what follows.

IV. PEZ And REM Based Schemes

From our previous discussion it is clear that we cannot approximate the cumulative CR interference with a simple distribution. The availability of such a result would have helped in calculating, for example, an exact expression for the exclusion zone radius in PEZ schemes or the number of allowable CRs in the REM based techniques. This would have further shed light on the dependence of system performance on various different parameters. Hence, as a first look at this problem we study various CR scheduling schemes based on results obtained by computer simulations. We also stress here that we do not deal with the issue of how the CRs would communicate with each other and pass on the information about their activity as this is beyond the scope of the current work. This, for example, can involve the CRs communicating with a controller upon getting a go ahead for using the spectrum. In all simulations CRs are located uniformly in the primary coverage area. The number of active CRs, N_{CR}, is binomially distributed [3] with a maximum number of CRs given by $\pi R^2 D_{CR}$, where D_{CR} is the density of the CRs (number of CRs per m^2) and we ignore the negligible hole in the circle of radius R_0. The binomial probability that a CR wishes to transmit is given by the activity factor, $p = 0.1$. The primary receiver is at the center of the coverage area and the primary transmitter is also uniformly located in the primary coverage area. In this section we consider two fundamentally different schemes for managing the interference at the PU receiver. The REM approach utilizes complete knowledge of all the interference values whereas the PEZ approach only uses average information of all interferers within a certain distance of the PU receiver. Assume there are N_{CR} CR transmitters which desire a connection. Each of the N_{CR} CRs has an interference power at the primary receiver given by (1) and denoted $I_1, I_2, \ldots, I_{N_{CR}}$. Based on these interference values, the PEZ and REM approaches are described below.

[3]We mention that to arrive at (19) we used a Poisson variable to model the interfering CRs (in the limiting case when the number of CRs tends to infinity and the probability of each interfering CR is small enough) for the sake of mathematical tractability. Here, without loss of generality, we assume a binomial random variable modeling the finite number of such CRs.

A. PEZ Approach

In contrast to a REM approach that uses a detailed REM to give information about the interference resulting from any CR, the PEZ approach [10] only uses location information to control the access of CRs. A simple exclusion zone is created with radius R_e around the primary receiver. No CR is allowed to transmit inside the PEZ and all CRs outside the PEZ are permitted. The radius, R_e, is set so that the cell-edge SINR is degraded by a certain amount. Specifically, the primary coverage area is defined to give an SNR greater than 5 dB, 95% of the time. By allowing CRs to operate we accept a new SINR target, less than 5 dB, which is achieved at least 95% of the time.

B. REM Approach

The REM approach [11] assumes that $I_1, I_2, \ldots, I_{N_{CR}}$ are known and selects those CRs for transmission which satisfy an SINR constraint. The constraint chosen is that the added interference must not decrease the SNR by more than Θ dB. For example, if SNR = 10 dB in the absence of CRs, then those CRs chosen must give SINR $\geq (10 - \Theta)$ dB. Two methods are chosen for selection, a centralized approach and a decentralized approach.

- *Centralized Selection:* Here we assume that a centralized controller knows $I_1, I_2, \ldots, I_{N_{CR}}$ instantaneously and creates a list of the ordered interferers as $I_{(1)} \leq I_{(2)} \leq \ldots \leq I_{(N_{CR})}$. The first n CRs are selected such that $\sum_{i=1}^{n} I_{(i)} \leq \Theta$ dB and $\sum_{i=1}^{n+1} I_{(i)} > \Theta$ dB.
- *Decentralized Selection:* Here we assume that the CRs are considered in their original order which can be interpreted as their order of arrival. Each interferer is considered in turn and is accepted if the combined interference from previously accepted CRs and the current CR is less than Θ dB. If a CR is not accepted, the next CR in the list is investigated.

The usefulness of REM based techniques hinges around the quality of the information available. Thus we discriminate between perfect and imperfect REM information in the following.

1) A Perfect REM: A REM can hold a wide variety of information [21] and it is not clearly understood at present what constitutes a practical and effective REM. In this work we assume that the REM contains signal strength data. In a perfect REM the signal strength from all source coordinates to all destination coordinates is known. With this perfect REM a CR controller [1] can select those CRs for operation which satisfy a given interference constraint. The CR controller requires positional information for the PU and

the CRs, and can then use the REM to compute the overall SINR of the PU where

$$\text{SINR} = \frac{S}{\sum_{i=1}^{N} I_i + \sigma^2}. \tag{23}$$

In (23), S is the signal strength of the PU, σ^2 is the noise power and $\sum_{i=1}^{N} I_i$ is the aggregate interference of the N selected CRs. The interference constraint used is that the CR interference must not reduce the PU SNR by more than 2 dB. All results shown in the paper are for a 2 dB buffer. The value of 2 dB was chosen arbitrarily.

2) Modeling of REM Imperfections: In practise a perfect REM is impossible and for practical purposes the REM information is discretized in the form of a grid of points with grid size, Δ. Hence, the central controller allocating CRs will formulate its decisions on the basis of REM information obtained from the grid points, rather than from exact signal strength data. Hence, an interfering signal strength, I, will be estimated by $\hat{I}$ from the REM. The estimate is obtained from the grid-to-grid path in the REM which is closest to the actual signal path.

We consider the CR signal strength to be of the form given in (1). The REM predicted signal strength is given by

$$\hat{I} = Be^{\hat{X}}\hat{r}^{-\gamma}, \tag{24}$$

where $\hat{r}$ is the distance between the transmitter and the receiver in the REM grid and $\hat{X}$ is correlated with X by

$$\hat{X} = \rho X + \sqrt{1-\rho^2}E. \tag{25}$$

In (25) E is i.i.d. with X. Assuming a distance, d_i, between the actual and REM based position of the CR and a distance, d_p, between the actual and REM based location of the PU receiver, the correlation coefficient ρ can be obtained using an extension of Gudmundson's model [22] as

$$\rho = 0.5^{d_i/D_d} \times 0.5^{d_p/D_d}. \tag{26}$$

In (26) D_d is the so called *decorrelation distance* i.e., the distance at which the correlation between X and $\hat{X}$ drops to 0.5. The effect of flawed REM information on the signal strength between the primary transmitter and its receiver can be modeled using (24), (25) and (26). Simulation results of this model based on parameter values of a suburban macrocellular environment are given in Section V.

Optimal Interpolation: The above models for REM imperfections allow the effects of errors in the REM

to be simulated. However, REM accuracy is of key importance as shown in Sec. V and so it is useful to take a closer look at this issue. In what follows we derive the distribution of the errors resulting from the imperfect REM under certain idealized conditions.

Consider a REM with grid size, Δ, where the receiver is exactly located at one grid point and the transmitter location, P, is arbitrary, falling in one square of the grid pattern. We further assume that the signal strength model in (1) is exact and that, B, r, γ are exactly known. Hence, only the shadow fading is unknown and this information is exactly known at the grid points. We further assume that Gudmundson's model (26) holds with $d_p = 0$. Clearly this situation is extremely optimistic and leads to a lower bound on realistic REM errors. Now consider the signal strength from P to the PU receiver where P falls inside one of the grid boxes. Since all the five points (the four corners of the box and P) experience correlated shadow fading, we model the correlation between the normal random variables, X_i, associated with the lognormal shadowing at the five points using Gudmundson's model [22]. Thus,

$$\rho(X_i, X_j) = a^{d_{ij}}, \qquad i, j = 1, \ldots, 5, \tag{27}$$

where $\rho(X_i, X_j)$ represents the corrrelation between X_i and X_j, and d_{ij} is the distance between X_i and X_j. Using Gudmundson's results we choose $a = 0.998$ for suburban environments and $a = 0.886$ for urban environments. Furthermore, we assume that X_1 to X_4 form the corner points of the square with the principal diagonal between X_1 and X_3 and the other diagonal between X_2 and X_4. Hence, we have the following correlation matrix for $(X_1, \ldots, X_5)^T$:

$$\mathbf{R} = \begin{bmatrix} 1 & r & r^{\sqrt{2}} & r & r^{d_1} \\ r & 1 & r & r^{\sqrt{2}} & r^{d_2} \\ r^{\sqrt{2}} & r & 1 & r & r^{d_3} \\ r & r^{\sqrt{2}} & r & 1 & r^{d_4} \\ r^{d_1} & r^{d_2} & r^{d_3} & r^{d_4} & 1 \end{bmatrix}, \tag{28}$$

where $r = a^{\Delta}$, $\rho(X_5, X_i) = a^{d_i \Delta} = r^{d_i}, \forall i$ and d_i is the distance from the point P to the ith corner of the square. Performing the Cholesky decomposition we have $\mathbf{R} = \mathbf{A}\mathbf{A}^{\dagger}$, where $\mathbf{A}$ is a lower triangular matrix. Clearly, $\mathbf{A}$ can be factored as,

$$\mathbf{A} = \left[\begin{array}{c|c} \mathbf{A}_{11} & \mathbf{0} \\ \hline \mathbf{a}^T & b \end{array}\right], \tag{29}$$

where $\mathbf{A}_{11}$, $\mathbf{0}$ and $\mathbf{a}^T$ represent a sub-matrix, a column vector of zeros and a row vector of appropriate sizes respectively. Further, b represents a scalar lying between 0 and 1. With this notation, it can be shown that,

$$X_5 = \mathbf{a}^T \mathbf{A}_{11}^{-1} \begin{bmatrix} X_1 \\ X_2 \\ X_3 \\ X_4 \end{bmatrix} + bu_5, \tag{30}$$

where u_5 is $\mathcal{N}(0, \sigma_x^2)$. The first term in (30) represents the optimal estimator of X_5 using the REM and the second term gives the estimation error which is $\mathcal{N}(0, b^2\sigma_x^2)$. Note that this is standard theory [23]. Further it is worth emphasizing that this analysis can easily be extended to interpolation using more than 4 REM grid values.

It is evident that the performance of the above scheme heavily depends on the behavior of the error term which in turn relies on Δ and σ_x. One way to evaluate this is to compute the probability of underestimating signal strength (interference) from the CR devices. Based on (27)-(30) the probability of underestimating the interfering signal strength by an amount, E, is given by

$$\begin{aligned} P_E &= \text{Probability of underestimating the signal strength by more than } E \text{ dB} \\ &= P(\text{estimation error} < -E \text{ dB}) = Q\left(\frac{E}{b\sigma_x}\right), \end{aligned} \tag{31}$$

where $Q(.)$ gives the tail probability of a standard Gaussian. Hence, the Cholesky decomposition of $\mathbf{R}$ gives b which directly leads to (31), a simple closed form result for the effects of imperfect REM.

V. Simulation Results

Unless otherwise stated, we assume a PU coverage radius of $R = 1000$ m, and the transmit power is adjusted such that the SNR at the cell edge is 5 dB (i.e., in the coverage area the SNR exceeds 5 dB with probability 0.95). The CR transmit power is also chosen to meet a cell edge SNR of 5 dB for a given CR coverage radius, $R_c = 100$ m. Two kinds of CR penetration densities were chosen, a high density of $10,000$ CRs per sq. km and a corresponding moderate density of 1000 CRs per sq. km. Additionally, it was assumed that only 10% of the CRs wish to be active at any one time. The values of the propagation constants, γ and σ are given on the relevant figures. The shadow fading variance and path loss exponent should be taken as 8 dB and 3.5, respectively, when they are not explicitly mentioned. We stress that we

do not incorporate the effect of multipath fading in our simulations. Such an effect from the perspective of exploring second order characteristics was studied in [24].

A. Exclusion Zone Results

Given a variety of target SINRs, Fig. 2 shows the PEZ radius for different values of σ. For example, if the interference degrades the target SNR from 5 dB to an SINR of 4 dB, then the PEZ radius is approximately 700 m, for $\sigma = 6$ dB and $\gamma = 3.5$. It is interesting to note that the PEZ radius excludes virtually the entire PU coverage area for all target SINRs in $[0, 5]$ dB when $\sigma = 12$ dB, corresponding to dense urban areas. This result implies that for a given target SINR, environments with larger σ will result in higher interference and an increased R_e. This observation is consistent with previous observations reported in [25].

Increasing the CR transmit power or increasing R_c will correspondingly increase the interference and hence the PEZ radius. Figure 3 shows the PEZ radius vs target SINR for three different values of R/R_c. Reducing the CR transmit power will obviously result in a lower PEZ radius.

B. Comparison of Numbers of CRs

Figure 4 shows CDFs of the number of CRs for the two different types of REM approaches and the impact of varying the fading parameters. We observe that the centralized approach is superior, since it is designed to pick up the maximum number of CRs that aggregate to make up the acceptable interference degradation. We also note from Fig. 4 that increasing γ increases the number of permissible CRs. This is because environments where $\gamma = 4$ will experience less interference compared to environments where $\gamma = 3$ due to increased path loss. Similarly, simulation results showing the performance of the proposed REM based schemes with respect to σ variation were also obtained (not shown on account of space constraints). It was observed that increasing σ decreases the permissible number of CRs. This result reinforces the conclusion of Fig. 2 where increasing σ increased the PEZ radius - effectively reducing the area in which CRs operate and also reducing the permissible number of CRs. Note that dense urban environments are characterized by γ values of 4 and above and σ values of 8 dB and above. These two parameters have opposing effects on the permissible number of CRs.

Figure 5 compares the PEZ and REM approaches in terms of the percentage of CRs that gain access in a medium density environment. Here centralized approach is found to be the most superior, showing the

potential advantage gained if the CRs know the radio environment.The decentralized [4] approach shows a considerable advantage over the PEZ approach for higher values of the CDF. In addition to this, we also investigate the case of CRs with different coverage areas. In particular, we consider a coverage circle with radius uniformly distributed in [50 m, 150 m]. Such scenarios may correspond to heterogenous CR systems with application specific coverage zones. Clearly, in this case the mean value of the number of CRs given access remains nearly the same as before in the two REM based schemes. However, as expected, the variation in the percentage of CRs given access tends to increase.

The results in Figs. 4-5 taken collectively are important in a sense that they clearly show the advantage in terms of permissible CR numbers if a knowledge of the radio environment is made available to the CRs. Furthermore, they show that the full REM gains are only obtained if a smart access control algorithm is used which chooses many CRs with low interference instead of a few stronger interferers which might subsume the interference budget.

C. Imperfections in the REM

In practice, the radio environment is often modeled by dividing an area into a regular grid (typically composed of 100 m $\times$ 100 m grid boxes) and assuming that the fading conditions in any grid box can be approximated by a single point at the center of the box. For example, drive testing of cellular networks to validate path loss models and predicted signal coverage follows this approach. Clearly, larger grid sizes result in errors between measurement and prediction. On the other hand, reducing the grid size results in a large data overhead. Figure 6 shows the CDF of the magnitude of the actual CR-PU interference when the REM is estimated via a grid size ranging from 1 m $\times$ 1 m to 100 m $\times$ 100 m. The REM approach aims to maintain a 2 dB SINR buffer for the primary, but this is only possible with a perfect REM. When $\Delta = 1$ m the 2 dB buffer is nearly achieved (exceeded only 13% of time) but for a grid size of 50 m $\times$ 50 m, the interference exceeds 2 dB for approximately 70% of the time. For a grid size of 100 m $\times$ 100 m, 2 dB is exceeded 85% of the time and 5 dB is exceeded 10% of the time. In effect this means that if REM information is derived from a coarse grid, the buffer size must be increased or the CRs must back off from the buffer.

The effects of increasing the buffer or backing off the CRs are shown in Figs. 7 and 8 respectively. In Fig. 7 the PU has a target 2 dB buffer but due to the imperfect REM it will not always be achieved. Hence,

[4]We note that the decentralized approach performs worse than the centralized one as few CRs can consume the permissible interference budget (2 dB in this case).

an extra buffer is permitted beyond which the CRs are only allowed, 5% of the time. In Fig. 7 this scenario is denoted by the legend, Threshold = (original + extra) dB. The effects of spatially correlated shadow fading are also considered in Fig. 7. Shadow fading is correlated over any given area and the level of this correlation has a simple effect on the REM grid size. For highly correlated areas a coarse grid (large Δ) will be acceptable whereas in areas of low correlation, a fine grid (small Δ) will be required. Figure 7 shows the REM grid size vs the decorrelation distance of the shadow fading. For a given interference degradation (say the buffer value plus an additional 2 dB) a large decorrelation distance (say 500 m) enables a coarser grid size 130 m $\times$ 130 m relative to a decorrelation distance of 100 m (typical for dense urban areas) when the grid size is 38 m $\times$ 38 m.

In Fig. 8 we consider a back off in the CR allocation policy. In order to meet the nominal 2 dB SINR buffer at least 99% of the time, the CRs have to target a reduced buffer which is less than 2 dB. Figure 8 shows this buffer vs Δ for various values of D_d. For a grid size of 25 m $\times$ 25 m and a decorrelation distance of 100 m, the interference buffer is 0.88 dB. Figures 7 and 8 are instructive in determining the grid sizes for different radio environments.

To study the effect of interpolating signal strength from the position of a source point in a REM grid, we simulate the estimation error introduced in Sec. IV for different environments. In particular, we plot the probability of this error being less than a threshold of -3 dB (i.e., when we underestimate the interference by more than 3 dB) for urban and suburban environments based on meshes of 4 and 16 points for shadow fading variances of 6 dB and 12 dB as shown in Fig. 9. It is clear from the figure that interpolating the signal strength using the nearest 16 points in the REM grid is no better than using the closest 4 grid points. Furthermore, it is seen that owing to smaller decorrelation distances, finer grid sizes would be needed in urban environments ($a = 0.886$). In addition to this, shadowing has a negative impact on the performance of such REM systems in terms of underestimating the true interference produced by the CRs. The scale of the underestimation problem can be seen from a few examples in Fig. 9. In urban environments with 6 dB shadowing, 30% of time the interference is underestimated by more than 3 dB for a grid size of 31.6 m. Even with a much smaller 10 m grid this probability is still greater than 20%. Hence, despite underestimating the real REM errors, it can be seen that extremely small grid sizes may be needed to avoid harmful interference.

VI. Conclusion

The interference due to a single CR can be characterized in closed form for the scenario considered. However, the total interference due to multiple CRs is more difficult. Simple lognormal approximations are shown to be inaccurate and more complex models are required. Two interference management approaches have been considered based on REM and PEZ ideas. The REM approach requires considerable higher overheads but can perform substantially better than the PEZ one. To achieve these gains an intelligent allocation method is essential since providing access to CRs on a first-come-first-served basis can be worse than the PEZ method. However, the PEZ approach results is large exclusion zones especially for high σ and large R_c values. We have shown that interference degradation to the PU can be significantly underestimated if the channel state information needed to estimate interference levels is derived from a coarse REM. In particular, the probability of interference underestimation has been shown to be very high for urban environments. For practical deployments, this may mean that the PU has to accept a much larger interference from the CRs or the CRs may need to set a more conservative interference target. This will reduce the number of CRs allowed. The analytical work on lognormal deficiencies, user selection schemes and finite grid effects are the key, novel contributions.

References

[1] M. Hanif, M. Shafi, P. Smith, and P. Dmochowski, "Interference and deployment issues for cognitive radio systems in shadowing environments," in *IEEE International Conference on Communications (ICC)*, June 2009, pp. 1–6.

[2] M. Hanif, P. Smith, and M. Shafi, "Performance of cognitive radio systems with imperfect radio environment map information," in *IEEE Australian Communications Theory Workshop (2009)*, Feb. 2009, pp. 61–66.

[3] "Spectrum Policy Task Force Report (ET Docket-135)," Federal Communications Comsssion, Tech. Rep., 2002. [Online]. Available: http://hraunfoss.fcc.gov/edocs_public/attachmatch/DOC-228542A1.pdf

[4] M. A. McHenry, "NSF Spectrum Occupancy Measurements Project Summary," Shared Spectrum Company, Tech. Rep., 2005.

[5] D. Qu, Z. Wang, and T. Jiang, "Extended active interference cancellation for sidelobe suppression in cognitive radio OFDM systems with cyclic prefix," *IEEE Trans. Veh. Technol*, vol. 59, no. 4, pp. 1689 –1695, May 2010.

[6] D. Qu, Y. Yi, T. Jiang, and G. Zhu, "EM-based noise plus interference estimation for OFDM-based cognitive radio systems," *Wireless Commun. and Mobile Computing*, 2010.

[7] S. Haykin, D. Thomson, and J. Reed, "Spectrum sensing for cognitive radio," *Proc. IEEE*, vol. 97, no. 5, pp. 849 –877, May 2009.

[8] A. Ghasemi and E. Sousa, "Interference aggregation in spectrum-sensing cognitive wireless networks," *IEEE J. Sel. Topics Signal Process.*, vol. 2, pp. 41–56, Feb. 2008.

[9] X. Hong, C.-X. Wang, and J. Thompson, "Interference modeling of cognitive radio networks," in *Proc. IEEE Vehcular Technology Conference (VTC) Spring*, 2008, pp. 1851–1855.

[10] M. Vu, N. Devroye, and V. Tarokh, "On the primary exclusive region of cognitive networks," *IEEE Trans. Wireless Commun.*, vol. 8, no. 7, July 2009.

[11] Y. Zhao, D. Raymond, C. da Silva, J. Reed, and S. Midkiff, "Performance evaluation of radio environment map-enabled cognitive spectrum-sharing networks," in *Proc. IEEE Military Communications Conference (MILCOM)*, Oct. 2007, pp. 1–7.

[12] A. Goldsmith, *Wireless Communications*. New York: Cambridge University Press, 2006.

[13] L. Fenton, "The sum of lognormal probability distributions in scatter transmission systems," *IRE Trans. Commun. Syst.*, vol. CS-8, pp. 57–67, 1960.

[14] S. Schwartz and Y. Yeh, "On the distribution function and moments of power sums with lognormal components," *Bell Syst. Tech. Journal*, vol. 61, pp. 1441–1462, 1982.

[15] A. Abu-Dayya and N. Beaulieu, "Outage probabilities in the presence of correlated lognormal interferers," *IEEE Trans. Veh. Technol.*, vol. 43, pp. 164–173, Feb. 1994.

[16] N. Beaulieu, A. Abu-Dayya, and P. McLance, "Estimating the distribution of a sum of independent lognormal random variables," *IEEE Trans. Commun.*, vol. 43, pp. 2869–2873, Dec. 1995.

[17] N. Beaulieu and Q. Xie, "An optimal lognormal approximation to lognormal sum distributions," *IEEE Trans. Veh. Technol.*, vol. 53, pp. 479–489, Mar. 2004.

[18] N. Mehta, J. Wu, A. Molisch, and J. Zhang, "Approximating a sum of random variables with a lognormal," *IEEE Trans. Wireless Commun.*, vol. 6, no. 7, pp. 2690–2699, July 2007.

[19] Z. Liu, J. Almhana, and R. McGorman, "Approximating lognormal sum distributions with power lognormal distributions," *IEEE Trans. Veh. Technol.*, vol. 57, no. 4, pp. 2611–2617, July 2008.

[20] J. Kingman, *Poisson Processes*. New York: Oxford Univ. Press, 1993.

[21] Y. Zhao, L. Morales, J. Gaeddert, K. Bae, J.-S. Um, and J. Reed, "Applying radio environment maps to cognitive wireless regional area networks," in *Proc. IEEE International Symposium on New Frontiers in Dynamic Spectrum Access Networks (DySPAN)*, April 2007, pp. 115–118.

[22] M. Gudmundson, "Correlation model for shadow fading in mobile radio systems," *IEEE Electron. Lett.*, vol. 27, no. 23, pp. 2145–2146, 1991.

[23] H. Stark and J. Woods, *Probability and Random Processes with Applications to Signal Processing*. Prentice Hall, 2001.

[24] M. Hanif and P. Smith, "Level crossing rates of interference in cognitive radio networks," *IEEE Trans. Wireless Commun.*, vol. 9, no. 4, pp. 1283–1287, April 2010.

[25] A. Viterbi and A. Viterbi, "Erlang capacity of a power controlled CDMA system," *IEEE J. Sel. Areas Commun.*, vol. 11, no. 6, pp. 892–900, Aug. 1993.

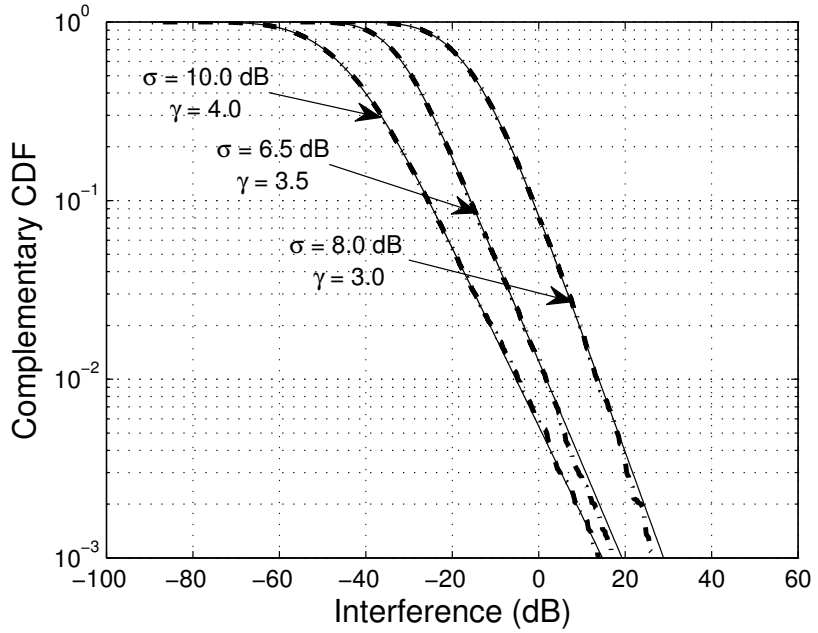

Fig. 1. A comparison of analytical and simulated complementary CDFs of interference over a range of propagation parameters. Solid lines represent analytical results while dotted-dashed curves show simulated values.

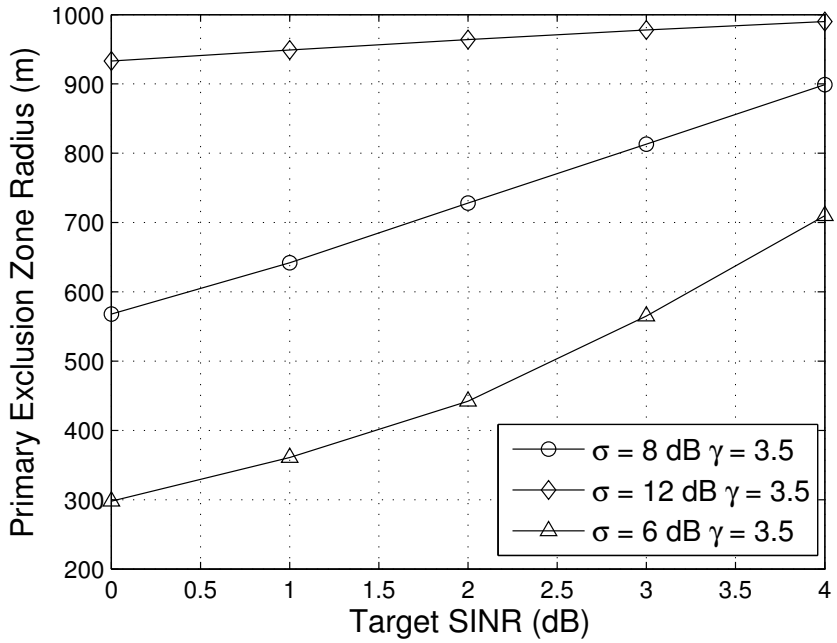

Fig. 2. The effect of σ and the target SINR on the PEZ radius for a medium density of CRs.

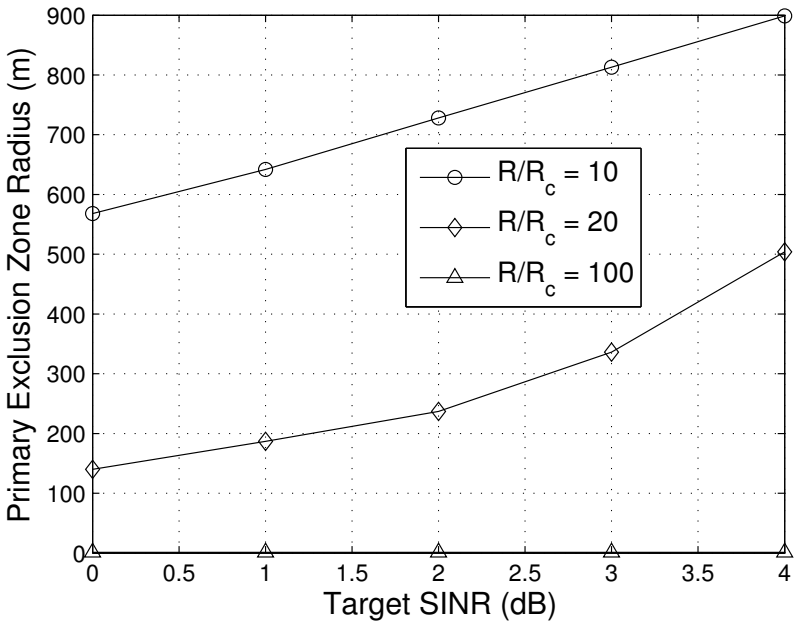

Fig. 3. PEZ radius vs target SINR for different values of the ratio of primary to secondary device coverage areas ($\sigma = 8$ dB, $\gamma = 3.5$).

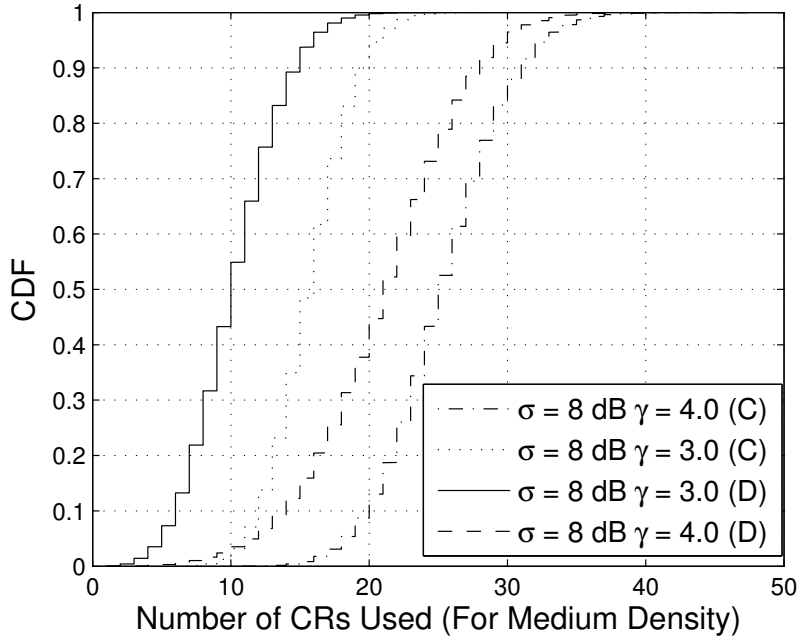

Fig. 4. CDF of the number of CRs obtained using REM based approaches for various γ values. D and C denote decentralized and centralized approaches.

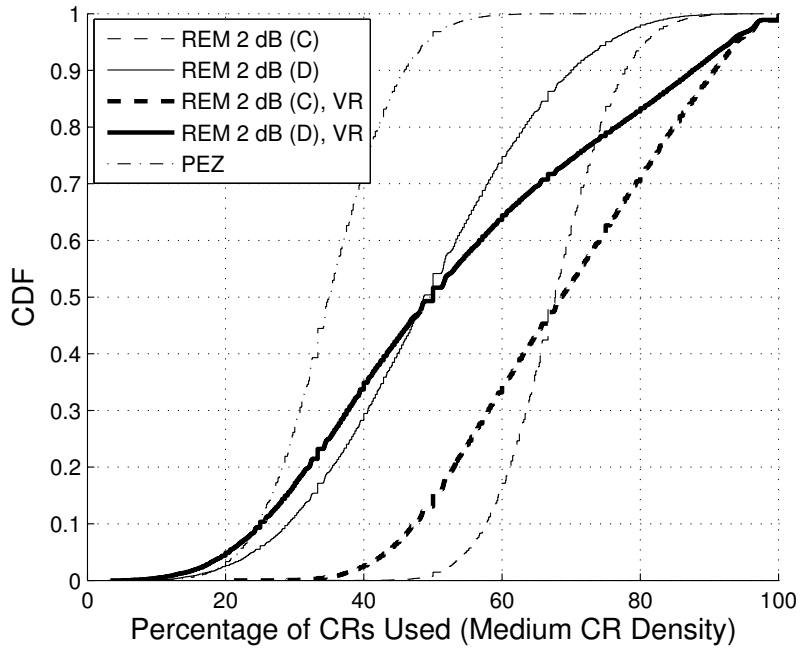

Fig. 5. Percentage of CRs given access for a medium CR density ($\sigma = 8$ dB, $\gamma = 3.5$). VR denotes a variable CR radius uniformly distributed between 50 m and 150 m.

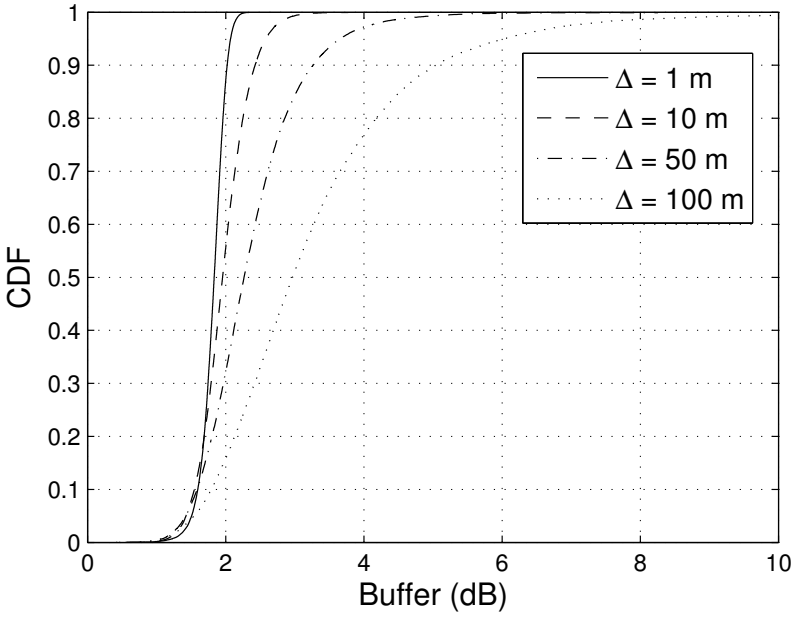

Fig. 6. Interference CDF for an REM enabled CR network for several values of Δ and decorrelation distance, $D_d = 100$ m.

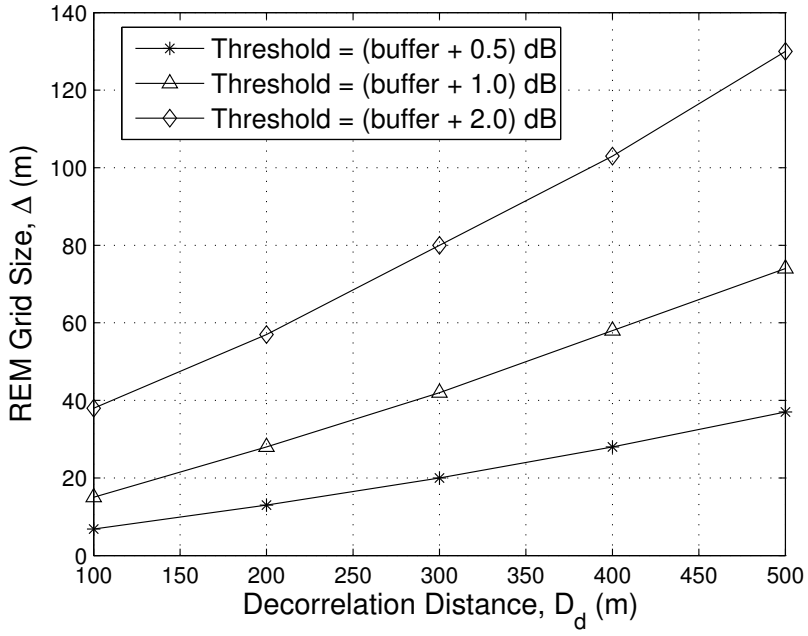

Fig. 7. REM grid size, Δ, vs decorrelation distance, D_d, for different threshold buffer sizes.

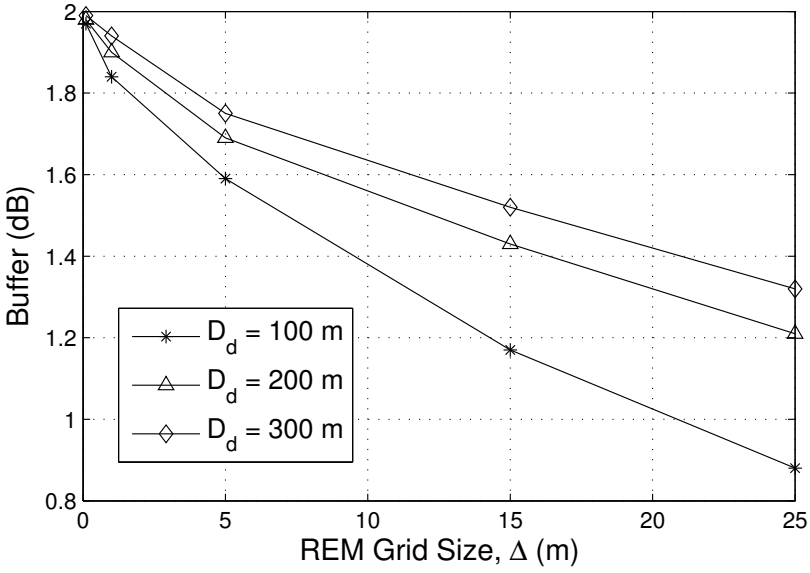

Fig. 8. Variation of actual buffer with REM grid size, Δ, for different values of the decorrelation distance, D_d.

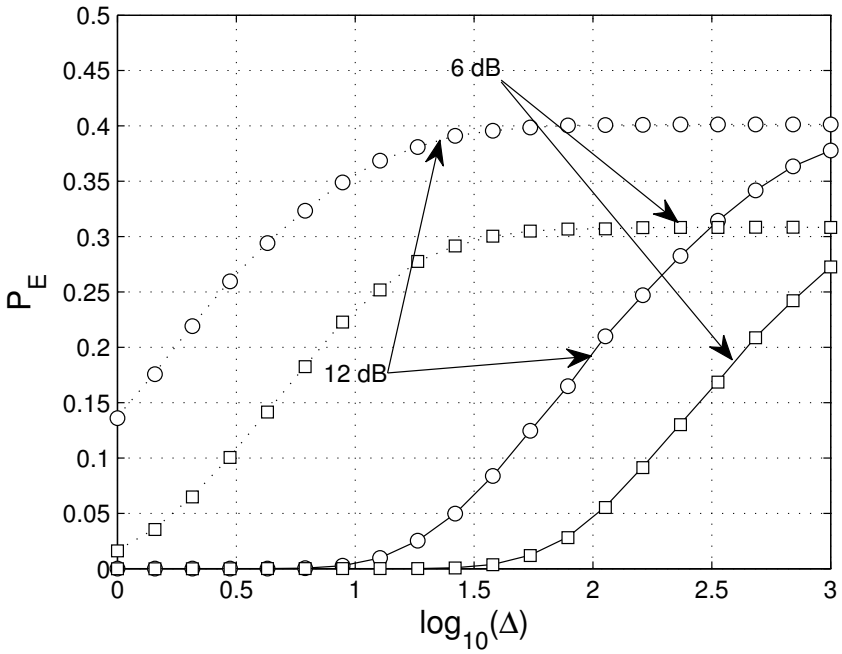

Fig. 9. Variation of the probability of underestimating the interference versus grid size. Solid lines are for suburban and dotted lines are for urban environments. The lines (solid and dotted) represent 4 point while the points (circles and squares) depict 16 point interpolation.